Theor. Appl. Climatol. 80, 229–243 (2005)
DOI 10.1007/s00704-004-0102-3

Theoretical and Applied Climatology
Printed in Austria

Institute for Atmospheric and Climate Science, Zürich, Switzerland

Modeling diurnal to seasonal water and heat exchanges at European Fluxnet sites

R. Stöckli and **P. L. Vidale**

With 8 Figures

Received October 27, 2003; accepted June 23, 2004
Published online December 15, 2004

Summary

The importance of linking measurements, modeling and remote sensing of land surface processes has been increasingly recognized in the past years since on the diurnal to seasonal time scale land surface–atmosphere feedbacks can play a substantial role in determining the state of the near-surface climate. The worldwide Fluxnet project provides long term measurements of land surface variables useful for process-based modeling studies over a wide range of climatic environments.

In this study data from six European Fluxnet sites distributed over three latitudinal zones are used to force three generations of LSMs (land surface models): the BUCKET, BATS 1E and SiB 2.5. Processes simulating the exchange of heat and water used in these models range from simple bare soil parameterizations to complex formulations of plant biochemistry and soil physics.

Results show that – dependent on the climatic environment – soil storage and plant biophysical processes can determine the yearly course of the land surface heat and water budgets, which need to be included in the modeling system. The Mediterranean sites require a long term soil water storage capability and a biophysical control of evapotranspiration. In northern Europe the seasonal soil temperature evolution can influence the winter energy partitioning and requires a long term soil heat storage scheme. Plant biochemistry and vegetation phenology can drive evapotranspiration where no atmospheric-related limiting environmental conditions are active.

1. Introduction

The interactions between the land surface and the atmosphere have been studied in a manifold way in climate research during the past decades. As described in Running et al. (1999) integrated approaches using tower flux measurements, satellite remote sensing and numerical modeling can help to understand the dynamics of the biosphere and land surface processes on various spatial and temporal scales. This approach has been used in major campaigns (e.g. FIFE: Sellers et al., 1988; BOREAS: Sellers et al., 1997b; LBA: Avissar et al., 2002). The exchange processes taking place at the land surface include short term feedbacks like vegetation transpiration controls over the bowen ratio (Chen et al., 2001); or radiation feedbacks through snow cover (Betts and Ball, 1997). On the seasonal time scale vegetation phenology (Bounoua et al., 2000; Buermann et al., 2001) and the soil moisture storage (Schär et al., 1999; Koster and Suarez, 2001) can play a role in the land surface hydrological cycle, especially through control of the boundary layer development and radiation-cloud-precipitation feedbacks. Soil heat storage and soil freezing in cold climates can play an important role in the land surface energy partitioning, as was found by McCaughey et al. (1997) and Viterbo et al. (1999). On the interannual or longer time scale feedbacks include processes like land use changes (Heck et al., 1999; Pielke, 2001) and nutrient cycling (Dickinson

et al., 2002). Many of these processes have been successively included in Land Surface Models (LSMs), which have been used in long term climate simulations and in numerical weather forecasting (Chen et al., 2001).

As reviewed by Henderson-Sellers et al. (2003) the land surface climate predicted from recent AMIP II (Atmospheric Model Intercomparison Project) GCM simulations is still strongly dependent on the used LSM and its parameter set, despite advances in modeling during the last decades. Long-term land surface observations are mostly not available on global scale for GCM-type comparison studies and this uncertainty limits their interpretation. There is also a need to know how biospheric measurements from global observational networks (e.g. satellite phenology) can be linked to processes modeled by LSMs. Integrations of such observational data have the potential to provide guidance to understand what is happening in coupled land surface–atmosphere climate simulations.

Following Sellers et al. (1997a) three generations of LSMs can be differentiated in terms of their complexity: first generation ''bucket'' models; second generation ''biophysical'' models; and recent third generation ''photosynthesis-conductance'' models. While the bucket approach is still used in some climate and numerical weather prediction models (see e.g. in Gedney et al., 2000), third generation models are already used in integrated ecosystem modeling (Cox et al., 2000; Eastman et al., 2001). Many LSMs in these three categories were also compared at the local scale, in off-line mode, by the PILPS (Project for the Intercomparison of Land-Surface Parameterization Schemes, Chen et al., 1997; Pitman and Henderson-Sellers, 1998) project and revealed a large spread among the models in terms of their heat and water fluxes, which helped to improve a number of LSMs. PILPS, however, aimed at comparing a large number of LSMs rather than at the analysis of individual schemes.

In comparison to PILPS, and following the categorization in Sellers et al. (1997a), this study uses three LSMs of increasing complexity (BUCKET by Manabe, 1969; BATS 1E by Dickinson et al., 1993; and SiB 2.5 (Sellers et al., 1996; Vidale and Stöckli, 2004)) shown in Fig. 1 to evaluate the aforementioned research questions at six European Fluxnet sites, distributed over three latitudinal zones (Mediterranean, central Europe, northern Europe). Each latitudinal zone includes one deciduous and one evergreen forest site (Fig. 2), so that the choice of these sites seeks to explore a substantial spread in climatic forcing and biomes. Fluxnet, a global network of micrometeorological measurement towers (Baldocchi et al., 2001), serves as an excellent driver and validatation data source for such a study since it provides multi-year and continuous data time-series in a standardized format. The analysis methodology of this study involves a comparison of the yearly course of modeled and measured soil temperature and soil moisture since these are prognostic variables in models and can control biophysical processes depending on climatic conditions. The insight into these processes then allows to compare and discuss resulting sensible and latent heat fluxes above the canopy, which are known to be largely LSM dependent.

The next section outlines the modeling methodology. In the results section modeled and

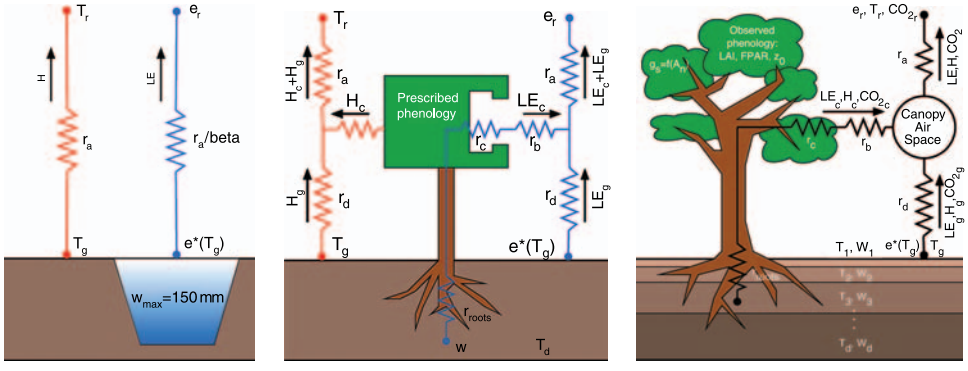

Fig. 1. Land Surface Model generations: BUCKET, BATS 1E and SiB 2.5

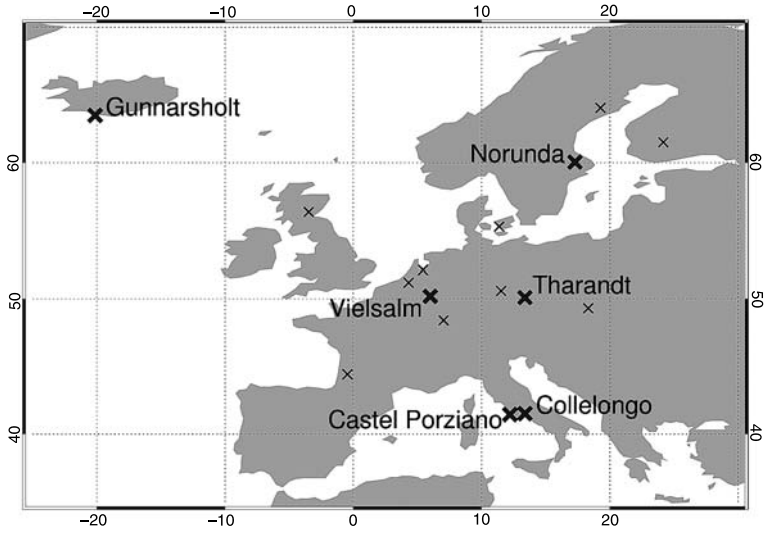

Fig. 2. Location of the European Fluxnet sites used in this study

observed soil temperature, moisture, heat and water fluxes are compared for the six Fluxnet sites. The discussion focuses on plant biophysical and soil storage processes and on finding important control mechanisms on surface fluxes in each climatic regime.

2. Methods

2.1 Data

Driver and validation data were both obtained from the Fluxnet project. The project uses standardized instrumentation to measure micrometeorological variables, water, heat, momentum and CO_2 fluxes, soil temperatures and moisture. The turbulent fluxes are measured using the eddy-covariance technique (Moncrieff et al., 1997) which can be sensitive to extreme climatic conditions, low wind speeds and heterogeneous terrain (Baldocchi et al., 2001; Schmid et al., 2003). Energy balance closure at Fluxnet sites, calculated from net radiation and eddy covariance sensible and latent heat fluxes, was estimated to be in the order of 20% (Wilson et al., 2002). This uncertainty in the data seems large, but its usability in a model comparison study can be justified: Fluxnet is the only continuously available global data for integrative biospheric research and our analysis will primarily focus on the time signature of fluxes and only secondarily on their magnitude.

The following Fluxnet data were used to drive the LSMs: short wave downward radiation (R_g [$\mathrm{W\,m^{-2}}$]), long wave downward radiation (LW_d [$\mathrm{W\,m^{-2}}$]), wind speed (WS [$\mathrm{m\,s^{-1}}$]), precipitation (PPT [mm]), surface pressure (P_s [Pa]), temperature (T_m [K]) and dew point temperature (T_d [K], or relative humidity RH [%]). Since data coverage of Fluxnet is around 65–75% (Baldocchi et al., 2001) the following gap-filling methodology was applied:

- short gaps (less than 6 hours) were filled with linear interpolation;
- longer gaps were filled with a 7-day running mean diurnal cycle of the missing variable;
- PPT gaps were not filled, except for the Italian station Collelongo, where precipitation was missing for the months January–July 1997. Precipitation values from a nearby reference station were used there.

LW_d is not distributed through the Fluxnet archive for the chosen measurement sites. It had to be parameterized using the radiation balance formulation:

$$LW_d = R_n - R_g + R_r + \epsilon\sigma T_s^4 \quad (1)$$

where R_n is the net radiation [$\mathrm{W\,m^{-2}}$], R_r is the reflected radiation [$\mathrm{W\,m^{-2}}$], ϵ is the land surface emissivity [–] (set to 1), σ is the Stefan Bolzman constant [$\mathrm{W\,m^{-2}\,K^{-4}}$] and T_s is the surface radiative temperature [K]. The latter was not available in the Fluxnet dataset but in a dense forest it will be close to the canopy temperature. A rough approximation was used by setting it to the mean of the soil surface and reference temperature, which should hold in the mean of the diurnal

cycle, as illustrated in Holtslag and Ek (1996). Using a radiative transfer scheme and a boundary layer parameterization to resolve T_s on the diurnal time scale was not feasible because these approaches are also dependent on LW_d. An uncertainty of ± 1 K in the used approximation results in an uncertainty in the order of 10 W m^{-2} in the derived radiation.

For cases where not all of the radiation components were available LW_d was derived empirically, by using the clear-sky LW_d formulation developed by Idso (1981). This formulation can however underestimate LW_d during cloudy days:

$$LW_d = \left(0.7 + 59.9 \cdot 10^{-6} q_m \exp\frac{1500}{T_m}\right)\sigma T_m^4 \quad (2)$$

where q_m is the water vapour pressure at reference height [Pa]. Gap filled surface fluxes corrected by Falge et al. (2001) are used in the results section. The yearly energy balance from observations at the Fluxnet stations is calculated as: $R_n = H + LE - G$ where LE, H and G are the latent, sensible and ground heat fluxes [W m^{-2}]. The yearly runoff R [mm] in observations is calculated as the residual of the water fluxes: $R = PPT - LE/L_v$ where L_v is the latent heat of vaporization [J kg^{-1}]. Soil temperature data at 30 cm depth and soil moisture data from TDR measurements were also used. The measurement depths of the latter data have been reported as follows: Collelongo 0–88 cm, Castel Porziano 40–70 cm, Vielsalm 45 cm, Tharandt 40–70 cm, Gunnarsholt 45 cm, Norunda 40–70 cm.

2.2 Models

BUCKET (Manabe, 1969) is a first generation model. It offers no biophysical control on water and heat fluxes except for a so called ''bucket'' which is able to hold precipitated water. The evaporation from this bucket is limited by the β factor [–] and has a linear dependence on soil moisture W [–] (relative to saturation):

$$\beta = f(W) \quad (3)$$

BUCKET requires few parameters (such as surface albedo or bucket size). The model used here is a modification of BATS 1E (Dickinson et al., 1993), including its thermal soil scheme, since the diurnal closure of the energy balance requires a ground heat flux. Any vegetation-related processes are turned off by setting the fractional vegetation cover to 0. The bucket-type evaporation is calculated by multiplying bare soil evaporation from a bucket with 150 mm water holding capacity with the β factor.

BATS 1E (Dickinson et al., 1993) is a biophysical model and it includes a bulk canopy layer that controls the water flux from the root zone to the atmosphere by regulating the stomatal conductance g_s [m s^{-1}], limited by environmental factors dependent on temperature T [K], soil moisture W [mm], water vapour pressure deficit (VPD) δe [Pa] and radiation PAR [W m^{-2}]:

$$g_s = f(PAR, \delta e, T, W) \quad \text{and} \quad g_c = g_s \cdot LAI \quad (4)$$

Canopy-scale fluxes are calculated by a linearly scaling with LAI (Leaf Area Index [m^2 m^{-2}]. LAI and other parameters depend on vegetation and soil type and are derived from look-up tables. Soil water is stored in a three layer soil (top, root, and deep soil) and soil heat is stored in a simple two-layer force-restore scheme.

SiB 2.5 (Sellers et al., 1996; Vidale and Stöckli, 2004) is a so-called photosynthesis-conductance model where plant transpiration is directly linked to net assimilation A_n [mol m^{-2} s^{-1}] by the Ball-Berry equation:

$$g_s = f(A_n) \quad \text{and}$$

$$g_c = \int_{z_1}^{z_2} f(V_{\max 0}, PAR) f(p\mathrm{CO}_2, \delta e, T, W) \Pi dz \quad (5)$$

Canopy-scale fluxes are calculated by expressing photosynthesis A_n as a canopy-integrated (from the canopy bottom z_1 to the canopy top z_2 [m]) function of radiation, nutrients ($V_{\max 0}$ [mol m^{-2} s^{-1}]), CO_2 pressure $p\mathrm{CO}_2$ [Pa], VPD, W and T. The PAR-use parameter Π [–] describes the extinction of light (and therefore nutrients and photosynthesis rate) through the canopy and is a function of $FPAR$ (Fraction of Photosynthetically Active Radiation available to plants), which controls both the phenological and biochemical activity. This framework requires less empirical parameters since $FPAR$ can be derived from spectral vegetation indices by satellite remote sensing. Water is stored in a three layer soil and a multi-layer thermal soil after Bonan (1996) and a new solution core including a prognostic canopy air space (CAS) as presented in this issue by Vidale and Stöckli (2004) is used.

Table 1. Model vegetation and soil boundary conditions

Site	Lat [°N]	Ion [°W]	Ref. height [m]	Vegetation type	Soil type
Collelongo	41.9	13.6	32	deciduous broadleaf	sandy loam
Castel Porziano	41.7	12.4	18	evergreen needleleaf	loamy sand
Vielsalm	50.3	6.1	40	deciduous broadleaf	loam
Tharandt	50.9	13.6	42	evergreen needleleaf	silt loam
Gunnarsholt	63.8	−20.2	2.5	deciduous shrub	sand
Norunda	60.1	17.5	100	evergreen needleleaf	loamy sand

The latter process allows for storage of heat, water and CO_2 in the air volume within the canopy.

2.3 Experimental set-up

The LSMs used in this study are forced at reference height (tower measurement height, Table 1) and with 30′ time-steps for an entire year (1997, except for Tharandt where 1998 offered a more continuous time series). The methodology did not involve any tuning of parameters to match measurements (similar to Baker et al., 2003) since it should reflect the use of LSMs coupled to distributed atmospheric models, where no such point-based tuning is possible.

All models were set up with the same initial soil thermal and hydrological conditions. Soil moisture layers were initialized at 50% of saturation. The soil surface temperature T_g was initialized with the first record of T_m and the deepest soil layer T_d was initialized with the yearly mean T_m. Any in-between thermal layers were linearly interpolated. Spin-up time for equilibrium was set to 5 years (after 2–3 years most sites did not show interannual change). The hydrological soil was divided into a 10 cm surface layer, a 90 cm root layer and a 3 m deep soil layer (except the bucket soil, which used a 150 mm soil water store). The SiB 2.5 multilayer soil heat scheme was divided into 6, 12, 24, 48, 100, 200 cm discrete layers.

Soil type and land cover class were the only prescribed parameters (Table 1) and were chosen according to Fluxnet site specifications and matched to the classes used by the LSMs. The models then created biophysical soil and vegetation parameters from the model specific look-up tables. In addition, SiB 2.5 vegetation parameters were derived by time varying satellite remote sensing NDVI (Normalized Difference Vegetation Index) as described in Stöckli and Vidale (2004).

3. Results

3.1 Soil moisture

Soil moisture measurements are generally difficult to compare with modeled values since soil properties vary by orders of magnitude on small spatial scales and they largely determine the scaling between volumetric water contents (measured) and absolute water contents (modeled). The analysis in this sub-section will focus on timing signatures and amplitude differences rather than on absolute soil moisture values.

In Fig. 3 the seasonal course of root soil moisture is plotted for the six Fluxnet sites. The soil moisture curves for the two Mediterranean sites show a large seasonal cycle, with a substantial depression during summer while at the other sites a shallower soil moisture cycle is observed. The measured soil moisture in Collelongo drops from around 60% in May to 20% in August and in Castel Porziano from 50% in February to less than 20% in August. For Collelongo SiB 2.5 is able to reproduce the winter values of this large seasonal cycle, but does not drop to the observed summer values. The soil moisture simulated by BATS 1E remains at a lower level and has an even shallower seasonal cycle. BUCKET, having no biophysical control on water transfer, runs out of water already in June and only begins to recharge the soil in October. SiB 2.5 and BUCKET recharge the soil moisture store to almost full saturation, but not BATS 1E. BUCKET also shows a heavy summer dryness in Castel Porziano. BATS 1E soil moisture performs well at this evergreen forest while SiB 2.5 does not show such a pronounced soil moisture depression like observed. Its winter soil moisture is again comparable to observations.

The two central European sites have a shallow seasonal soil moisture cycle and soil moisture

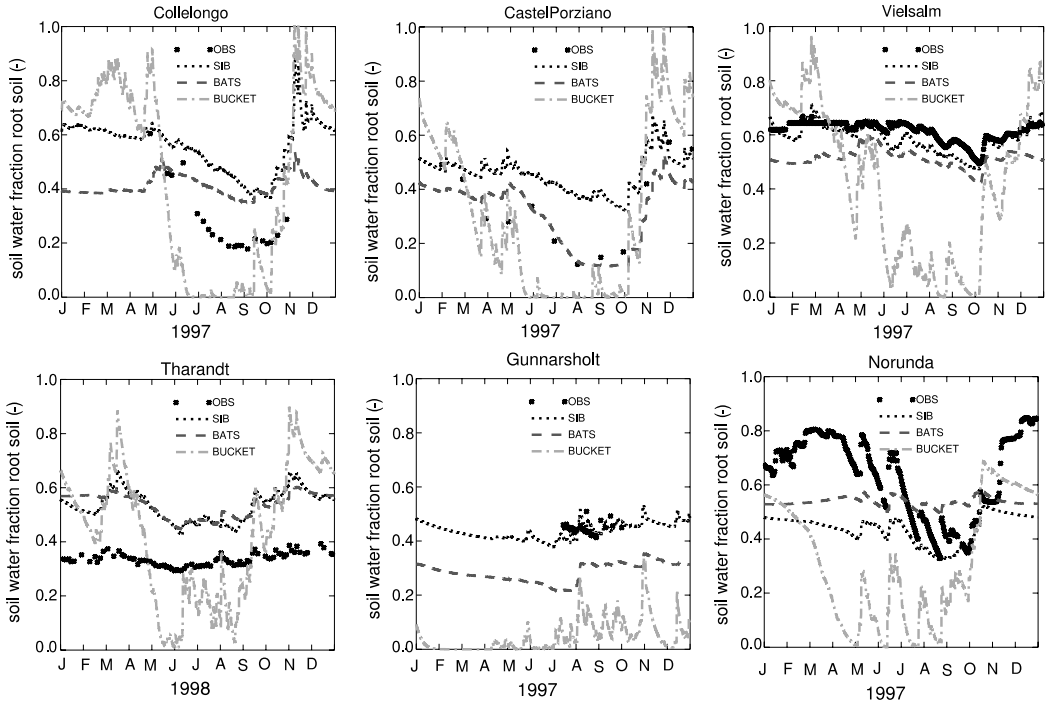

Fig. 3. Observed and modeled yearly root soil moisture

does not drop below critical values during summer. Again, the two models BATS 1E and SiB 2.5 are very similar and match observed soil moisture curves well for Vielsalm. Like in Collelongo BATS 1E exhibits a shallower cycle than SiB 2.5, which matches both the magnitude and timing of summer and winter values very closely. Both models overestimate the observed soil moisture by almost 20% at Tharandt, but the seasonal course of the soil moisture cycle is well represented. BUCKET shows a high soil moisture variability over the whole year, but summer precipitation is able to sustain the high evaporation needs of this simple model, so that the bucket never runs out of water like at the two Mediterranean sites.

The two northern European sites differ in their soil moisture cycle. A few soil moisture measurements are available for Gunnarsholt and BATS 1E and SiB 2.5 predict a shallow course in soil moisture at a high level while soil moisture in BUCKET constantly stays at a low level. The evergreen forest at Norunda shows a larger seasonal soil moisture cycle of similar magnitude (around 40%) like observed in the Mediterranean, but the soil moisture there does not drop to a critical level during summer. Observed spring values are almost at saturation – possibly due to snowmelt. Summer values modeled by both BATS 1E and SiB 2.5 are in the same range as observations, but spring and winter values are lower than observed. This result may be explained due to an inaccurate snow depth initialization in the steady-state simulation using a 5 year spin-up period with the same yearly forcing data.

Summarizing these results, the two models using a biophysical control on evapotranspiration (BATS 1E and SiB 2.5) generally show a shallower seasonal soil moisture course which matches better with observations. Especially at the two Mediterranean sites BUCKET simulates a soil moisture depression which is not in accordance with observations.

3.2 Soil temperature

Figure 4 shows observed and simulated soil temperatures at 30 cm depth. Soil temperature at this depth does not have much diurnal variation but can help to explain the seasonal course of the surface heat balance. The general picture over all sites reveals that soil temperatures are well simulated by SiB 2.5 during the summer period but overestimated by BATS 1E and BUCKET.

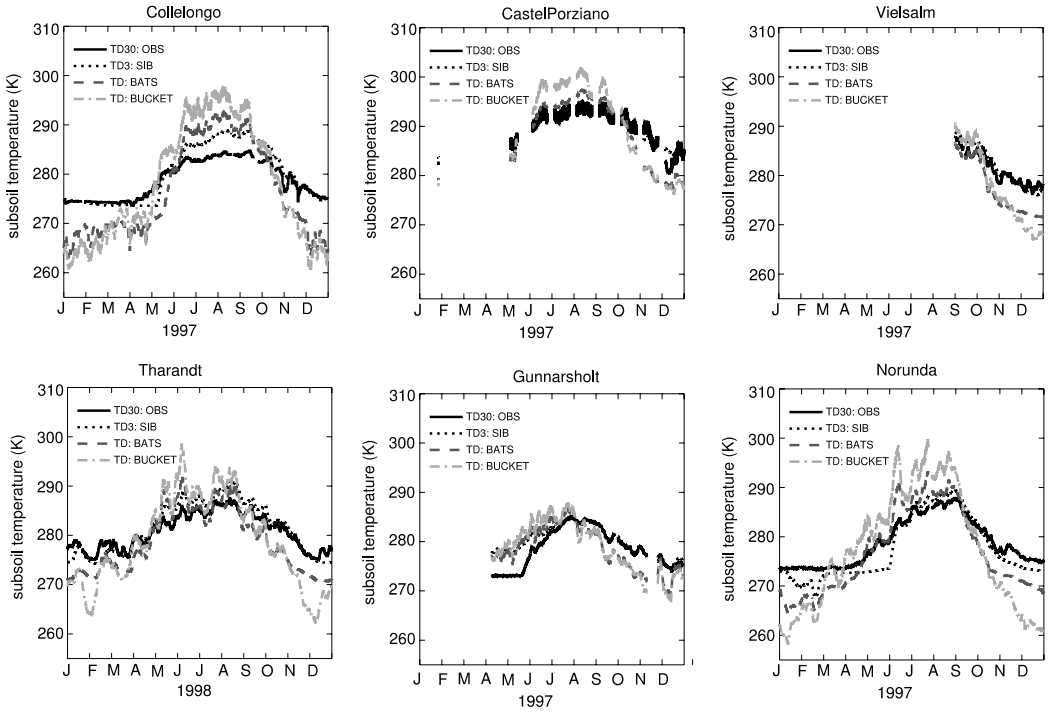

Fig. 4. Observed and modeled yearly soil temperature at 30 cm

During winter SiB 2.5 again shows a good agreement with observations but BATS 1E and BUCKET underestimate soil temperatures during this season. At Collelongo soil temperature stays at the freezing point during this period in SiB 2.5 but responds instantaneously to short term changes in atmospheric forcing in the other two models. Snow depth is not shown in the figures but BATS 1E and BUCKET have a 150 mm (120 mm, respectively) thick snow layer between January–June (10–50 mm in SiB 2.5) at this site. At Collelongo in particular all models overestimate summer soil temperatures by 5 K (SiB 2.5) or more (>10 K in BUCKET). The Mediterranean site Castel Porziano shows a reasonably good agreement between all models and observations during all periods. At this site soil temperature has a shallow seasonal course and always stays above the freezing point. In Vielsalm and Tharandt (in Vielsalm observations are limited to the September–October 1997) modeled summer soil temperatures are in good agreement with observations but only SiB 2.5 is able to reproduce the winter values which are above freezing in the observations.

BATS 1E and BUCKET underestimate the deep soil temperature by around 8 K at Gunnarsholt between September and December. BATS 1E performs better at Norunda: there only BUCKET largely underestimates winter soil temperatures by about 10 K.

The most prominent feature of SiB 2.5, with a multilayer diffusive soil heat transfer scheme, is that it is able to reproduce the seasonal course of the soil temperature at 30 cm much better than the force-restore soil heat scheme used in BATS 1E and BUCKET.

3.3 Heat and water fluxes

The differences in seasonal-scale soil moisture and temperature evolution shown in the previous two sub-sections can potentially control turbulent heat and water fluxes and the latter are analyzed in this section. Table 2 shows that the models simulate higher yearly mean *LE* than observed for Collelongo, the BUCKET being closest to observation and SiB 2.5 having the most evapotranspiration. *H* is underestimated by all models. Runoff compares well between models but is lower than derived from observations. In Figs. 5 and 6 the integrated *LE* and *H* fluxes are plotted. The plots allow to focus on the time signature of seasonal-scale fluxes rather than on absolute

Table 2. Mean net radiation (R_n), latent (LE), sensible (H) & ground heat (G), energy balance (BAL), runoff (R), evaporative fraction ($EF = \frac{LE}{H+LE}$) by site and model

	R_n [W m^{-2}]	H [W m^{-2}]	LE [W m^{-2}] ([mm])	G [W m^{-2}]	BAL [W m^{-2}]	R [mm]	EF [–]
Collelongo (Deciduous, precipitation 1997: 981 mm)							
OBS	83.5	43.3	19.9 (249)	−0.1	20.3	732	0.315
SiB	66.5	32.8	35.5 (444)	−1.8	0.0	557	0.520
BATS	71.3	36.6	33.9 (424)	1.8	−1.0	573	0.481
BUCKET	58.7	25.5	31.3 (392)	1.6	0.2	599	0.551
Castel Porziano (Evergreen, precipitation 1997: 399 mm)							
OBS	112.0	44.4	31.9 (399)	0.6	35.1	399	0.418
SiB	77.0	48.6	28.5 (357)	−0.1	0.0	323	0.370
BATS	80.2	31.3	49.4 (618)	−0.4	−0.1	57	0.612
BUCKET	68.1	30.4	38.1 (477)	−0.5	0.1	199	0.556
Vielsalm (Deciduous, precipitation 1997: 770 mm)							
OBS	71.7	24.4	24.6 (308)	0.2	22.4	462	0.502
SiB	54.2	23.1	30.3 (379)	0.6	0.0	392	0.567
BATS	61.6	18.0	45.6 (471)	−1.1	−0.8	211	0.717
BUCKET	56.2	10.7	47.5 (594)	−1.9	−0.1	180	0.816
Tharandt (Evergreen, precipitation 1998: 793 mm)							
OBS	61.2	23.4	37.6 (471)	−0.2	0.4	322	0.617
SiB	52.0	19.5	32.6 (408)	−0.1	0.0	387	0.626
BATS	59.0	6.4	55.8 (698)	−2.6	−0.6	95	0.896
BUCKET	57.5	1.9	58.0 (726)	−2.4	−0.1	78	0.969
Gunnarsholt (Deciduous, precipitation APR–DEC 1997: 471 mm)							
OBS	47.1	−6.1	18.1 (227)	0.9	34.2	320	1.770[1]
SiB	33.7	15.8	17.9 (224)	0.0	0.0	303	1.437[1]
BATS	37.6	−10.6	50.4 (631)	−1.2	−0.6	8	2.761[1]
BUCKET	36.9	−14.0	53.8 (673)	−3.2	0.2	0	2.420[1]
Norunda (Evergreen, precipitation 1997: 431 mm)							
OBS	59.7	12.7	29.6 (370)	0.0	17.4	61	0.700
SiB	57.9	38.4	19.8 (248)	−0.3	0.0	222	0.340
BATS	56.8	30.1	29.9 (374)	−2.9	−0.2	60	0.499
BUCKET	47.1	16.4	34.3 (429)	−3.4	−0.2	6	0.677

[1] Values >1 because of negative sensible heat fluxes

values (which is important due to a poor closure in the observed energy balance discussed in the methods section). The figures show that the seasonal course of LE and H at Collelongo is best represented by SiB 2.5, even though the integrated LE is much larger than observed. For this deciduous forest BATS 1E has no seasonal variation in its LE flux (large slope during the whole season) and BUCKET overestimates LE in spring and autumn and ceases evaporation during the whole summer (curve flattens during these months). Despite the inter-model differences in the seasonal course of LE the total yearly LE flux is very similar for all models. The timing of the diurnal course of LE and H during July (Figs. 7 and 8) matches best for SiB 2.5, followed by BATS 1E and BUCKET, the latter two underestimating the magnitude of LE during summer. Both models however show excessive LE and a depressed H during the other seasons.

In Castel Porziano the yearly mean LE flux has a substantial spread between models as can be seen from Table 2 the most complex model, SiB 2.5, comes closest to observations, underestimating evapotranspiration flux by 10.7%, where both BATS 1E and BUCKET overestimate LE by 54.9% and 19.4%, respectively. It can be seen from Fig. 6 that a good performance of the yearly

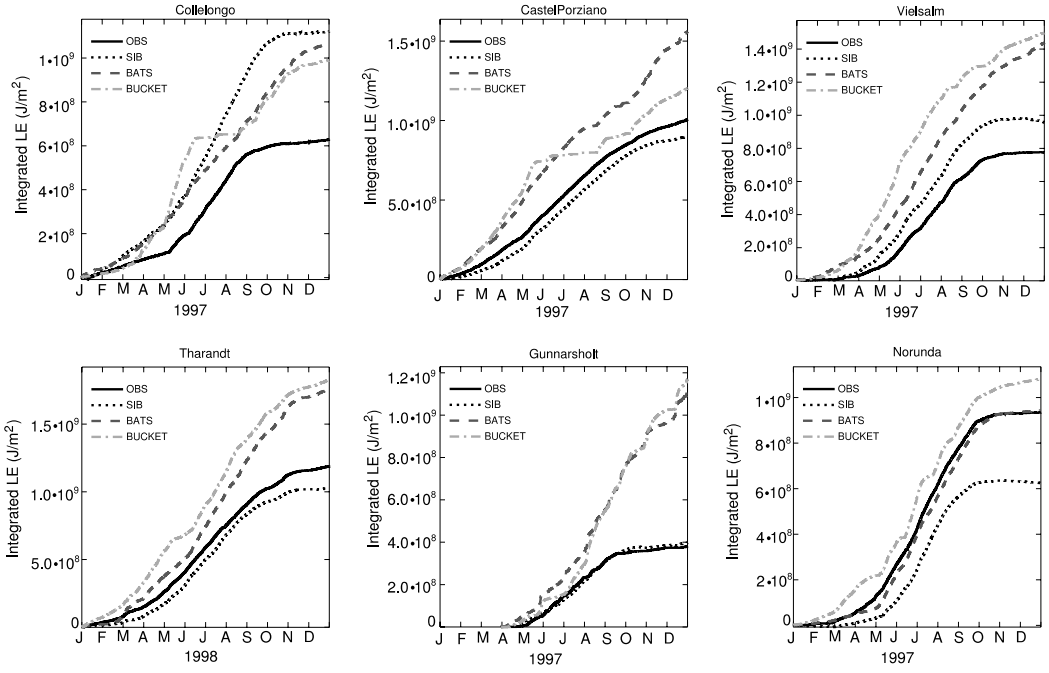

Fig. 5. Observed and modeled yearly integrated *LE* fluxes

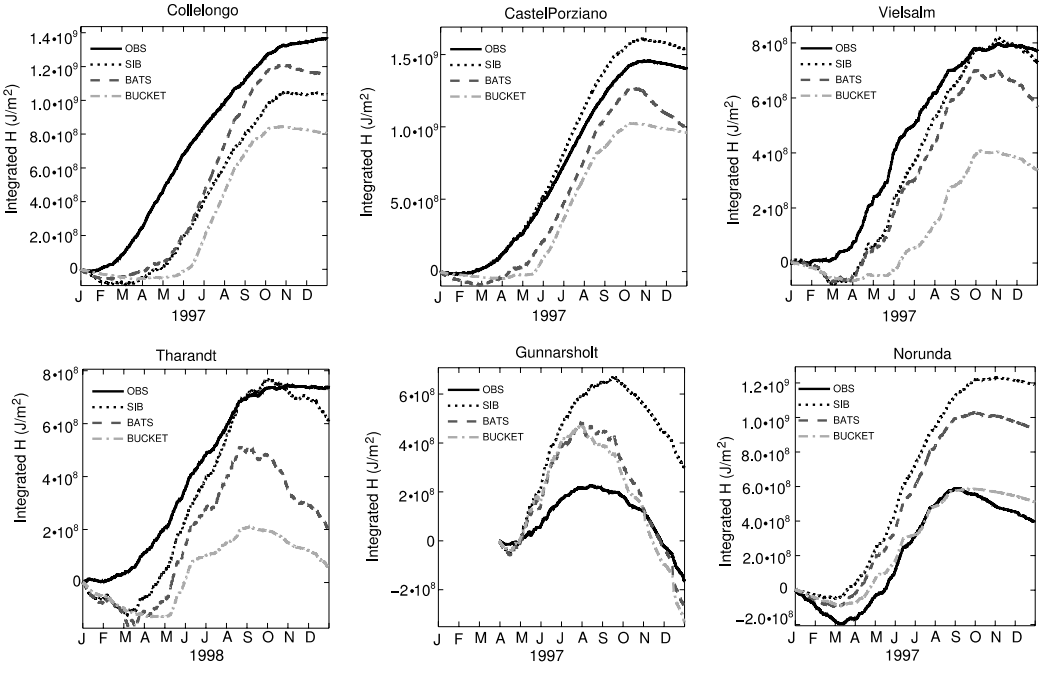

Fig. 6. Observed and modeled yearly integrated *H* fluxes

LE flux in SiB 2.5 also results in a good match of the yearly *H* flux while the overestimation of *LE* in BATS 1E results in underestimated *H*. BUCKET shows a similar summer *LE* anomaly like in Collelongo. Runoff is simulated well by SiB 2.5 and largely underestimated by BATS 1E and BUCKET.

The two central European sites Vielsalm and Tharandt are in the same latitudinal zone and the climatic conditions at both sites are comparable.

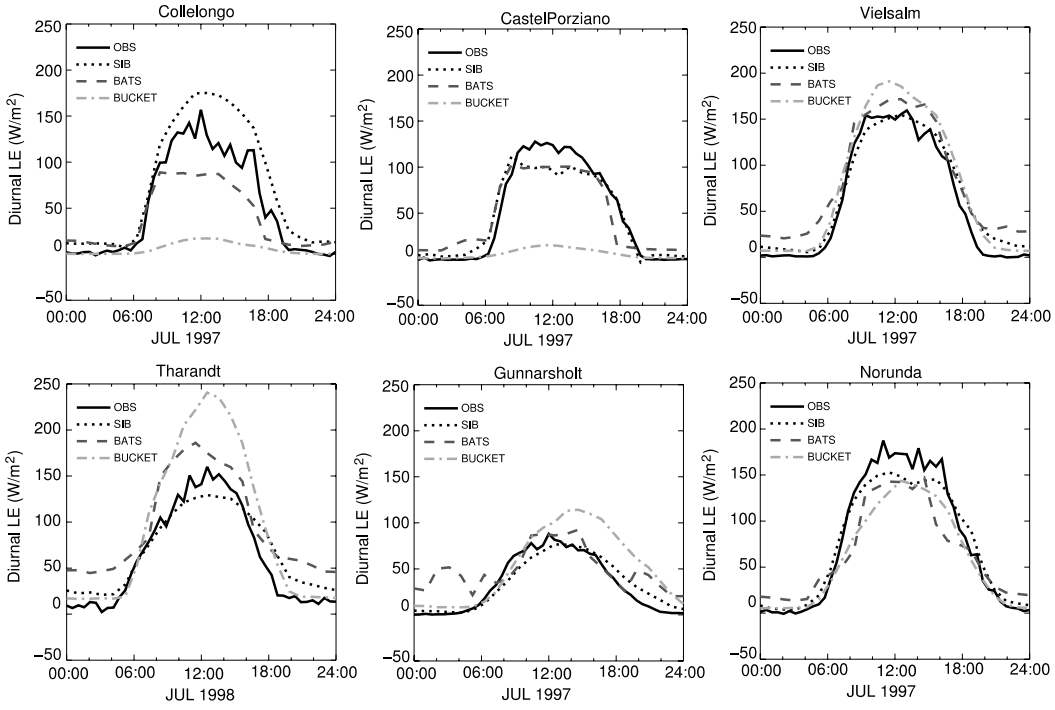

Fig. 7. Observed and modeled diurnal *LE* fluxes (July)

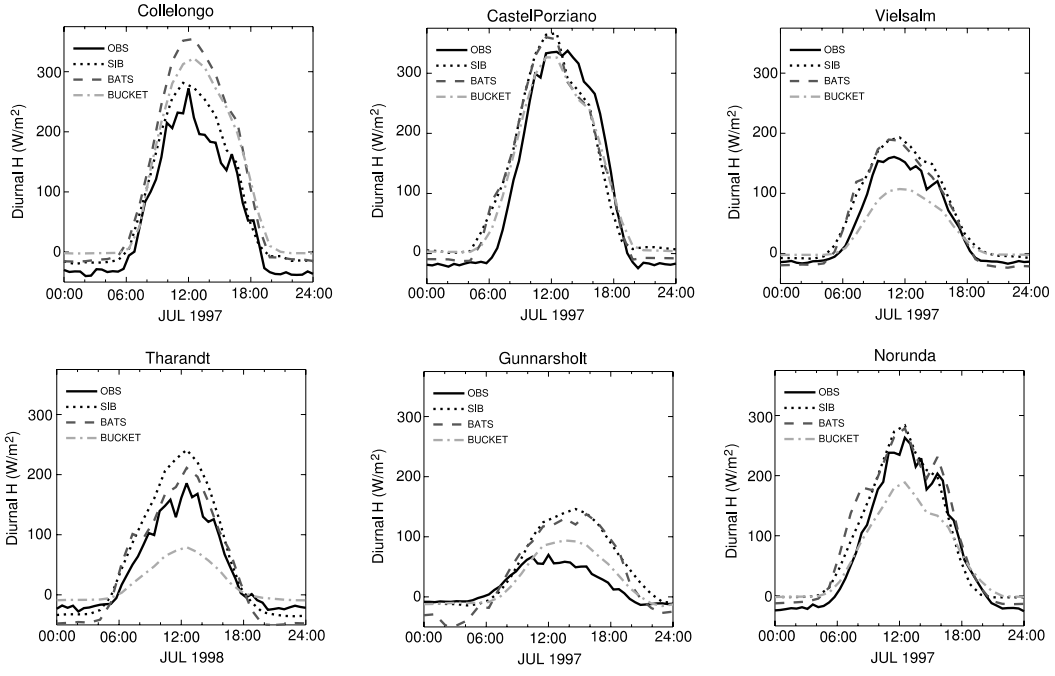

Fig. 8. Observed and modeled diurnal *H* fluxes (July)

SiB 2.5 shows a very good agreement to observations in yearly mean *H* and *LE* fluxes and also comes close to the observed evaporative fraction for the two sites. Both BUCKET and BATS 1E overestimate the yearly course of *LE* fluxes and underestimate *H* fluxes as this is shown in Figs. 5 and 6. At the evergreen forest at Tharandt BUCKET uses almost all available energy for evaporation resulting in an evaporative fraction close to unity. In Fig. 7 it can also be seen that

BATS 1E shows a displaced diurnal *LE* flux, even during night, which can explain its excessive yearly *LE* flux. Both, the timing and magnitude of the diurnal course of *LE* and *H* can be reproduced best with SiB 2.5. Runoff (Table 2) matches better with observations for the deciduous forest in Vielsalm than at the evergreen site; runoff is especially underestimated in BATS 1E and BUCKET for the evergreen forest.

Table 2 shows that Gunnarsholt receives the least net radiation of the six sites and observations show a negative mean sensible heat flux there. Both BATS 1E and BUCKET overestimate *LE* flux by a factor of 2.5, at the cost of only having little runoff. Again, the two models seem to use the available radiation for putting moisture into the atmosphere (Fig. 5) while SiB 2.5 is able to almost exactly reproduce the relatively small latent heat flux associated with the short growing season of this northern European deciduous plantation. A good representation of the *LE* flux in SiB 2.5 also gives a good match in runoff, but it overestimates the *H* flux – especially during summer. Similar results are seen for the evergreen site Norunda. The modeled *H* fluxes for Norunda are larger than observed. BATS 1E matches very well in *LE* fluxes and in runoff while SiB 2.5 underestimates *LE* and overestimates runoff. On the diurnal scale all models perform well at Norunda but show a poorer performance in Gunnarsholt. Especially BATS 1E cannot reproduce well the nighttime fluxes at Gunnarsholt and BUCKET overestimates the magnitude of the daytime *LE* flux.

4. Discussion

4.1 Mediterranean

A large inter-model variability of *LE* for the two Mediterranean sites Collelongo and Castel Porziano is seen on the diurnal and the seasonal time scale (Figs. 5 and 7). All three models come to roughly the same yearly total *LE* in Collelongo but during the growing season they each largely present their own solution as this was shown in the results section. Collelongo receives around $83.5\,\mathrm{W\,m^{-2}}$ of mean net radiation (Castel Porziano: $112\,\mathrm{W\,m^{-2}}$), and observations indicate that only 31.5% of this energy is transferred into latent heat (Castel Porziano: 41.8%). This fraction is much higher at central European sites (50.2% at Vielsalm and 61.7% at Tharandt). Such a high energy availability at the two Mediterranean sites results in a high atmospheric demand and requires a biophysical limitatation of the water transfer between the biosphere and the atmosphere and a sufficent soil water storage capacity to sustain this water flux during dry periods. BUCKET with no such regulation mechanism highly overestimates *LE* in spring and autumn, running out of water during summer, which is shown in the yearly soil moisture curves (Fig. 3). This model then overestimates soil temperatures in summer by around 10 K and has an exaggerated *H* flux (day and night) because it has no evaporative cooling during this period. In Castel Porziano BUCKET *LE* shows a similar seasonal course but there the difference between the biophysical model BATS 1E and the photosynthesis-conductance model SiB 2.5 is large. At this site precipitation in 1997 was 399 mm and much lower than at Collelongo (981 mm). The observed soil moisture curve therefore shows very low values during summer in Castel Porziano and BUCKET is strongly soil moisture limited during this period (but not BATS 1E and SiB 2.5, BATS 1E is however close to the wilting point) due to its lacking biophysical control on water transfer. The difference between the BATS 1E and SiB 2.5 *LE* fluxes can be explained with Eqs. (4) and (5). Evapotranspiration in both models are limited by T, δe, W and PAR and but at high atmospheric demands plant biochemistry in SiB 2.5 can also limit *LE*, which is the large difference between the two models. The photosynthesis process is driven by the availability of nutrients, light and the ability of the plant to use the photosynthesis products and since this process is not included in BATS 1E it highly overestimates the yearly integrated *LE* flux while observations and SiB 2.5 show an upper limit of around $1 \cdot 10^9\,\mathrm{J\,m^{-2}}$. The exaggerated *LE* of BATS 1E results in a larger soil moisture depression during summer, which is, however, better in accordance with observations. On the other side *LE* and *H* fluxes of SiB 2.5 at this site better compare with observations, which may put in question the observed soil moisture at this site. As already suggested the representativeness of absolute soil moisture values is not straight forward, considering the spatial heterogeneity of this variable.

4.2 Central Europe

At the two central European sites observed soil temperature is mostly above freezing and soil water has a very shallow seasonal course at a high mean level as shown in Figs. 3 and 4, therefore neither of these variables are largely controlling biophysical processes over the seasonal course. Rainfall totals to 770 mm in Vielsalm and 793 mm in Tharandt and does not show much seasonal variability. Yearly heat and water fluxes are best simulated by SiB 2.5 and the other two models overestimate *LE* and underestimate *H* for both sites resulting in an excessive evaporative fraction (Table 2) in these models. Due to the balanced environmental conditions at Vielsalm and Tharandt water fluxes of BUCKET (Eq. (3)) and BATS 1E (Eq. (4)) are only constrained by the diurnal course of *PAR* but not so much by *W*, *T* and δe. In this case, the SiB 2.5 transpiration still obeys to the maximum photosynthesis rate which is especially sensitive to nutrients (V_{max0}) and *PAR* (Eq. (5)). SiB 2.5 distributes these quantities through the vertical extent of the canopy by the use of an extinction function dependent on *FPAR* which obeys the seasonal course of phenology (also see Sellers et al., 1997a). The latter is especially important for the deciduous forest Vielsalm. Figure 5 shows that the seasonal course of *LE* is very well reproduced by SiB 2.5 (leveling to around $1 \cdot 10^9$ J m^{-2} in the yearly total, also in Tharandt) but not by the other two models (which show a low seasonality in their *LE* course). Their excessive *LE* fluxes result in depressed seasonal-scale *H* fluxes, also visible on the diurnal time scale in Figs. 7 and 8 for the BUCKET model. Furthermore *H* fluxes in BATS 1E are negative during stable conditions (night, morning, evening) and its diurnal *LE* course starts earlier than the one of SiB 2.5. As was shown in Vidale and Stöckli (2004) (this issue) the CAS storage capability in SiB 2.5 can support the storage of heat and water during times of low turbulence. At night this storage prevents excessive cooling of the surface layer and during transition times between stable and unstable surface layer stratifications it delays the start of turbulent fluxes, which is well demonstrated in the diurnal course of *LE* (Fig. 7) and *H* (Fig. 8) at Vielsalm and Tharandt.

4.3 Northern Europe

At the northern European sites a low amount of R_n is available for land surface processes during a short time period. At the Icelandic site Gunnarsholt BUCKET and BATS 1E almost completely use it for *LE* and even show a negative *H* flux in the mean (Table 2). Soil moisture is not limiting BUCKET evaporation at this site (Fig. 3) and the relatively mild air temperature in south-western Iceland is not controlling biophysical processes in BATS 1E. Due to a short growing season and the low amount of available energy only about half of the integrated *LE* is observed at this site compared to the others. Therefore plant biochemistry is not operating at its full capacity which means that SiB 2.5 photosynthesis limitation cannot explain why a more sound energy partitioning is seen in this particular model. Unlike for the other sites, where inter-model differences show up during summer, the main difference in the integrated *LE* fluxes are seen only after August. A large divergence between BATS 1E/BUCKET and SiB 2.5 is observed also in the *H* flux. The reason for this inter-model difference can be found by analyzing their thermal soil scheme. BUCKET and BATS 1E use a simple force-restore scheme (extending to around 1 m depth) and show a negative bias of up to 5–15 K in soil temperatures after August compared to observations, which transfer into negative sensible heat fluxes (since *H* is largely driven by radiation and the soil surface temperature) and exaggerated *LE* fluxes (since *LE* is mostly driven by radiation at this site). Only a diffusive 4 m deep thermal soil scheme used in SiB 2.5 is able to reproduce the soil temperatures correctly, resulting in a higher *H* flux. Radiation is limiting at Gunnarsholt outside the growing season and then the soil heat flux becomes an important driver for the partitioning between *LE* and *H* since *LE* is not driven by plant biophysics anymore. Soil temperatures simulated with the force-restore scheme also are underestimated at the other sites but there solar radiation and plant biophysics drive the surface energy balance during most of the year as this was shown in the previous two sub-sections. At Norunda for example, a longer growing period and a higher mean net radiation results in a 2.5 times higher *LE* than at Gunnarsholt. There all models show skill in

representing the seasonal course of *LE* flux (BATS 1E being closest to observations) since the seasonal course of *LE* is mostly driven by *PAR* and *T* (winter) but not to a large extent by the other factors in Eqs. (3)–(5).

5. Conclusion

In this study, three land surface models of different complexity were applied at six European Fluxnet sites. Processes of soil moisture and heat storage and their biophysical interaction with seasonal-scale land surface fluxes were analyzed. The focus was not in obtaining the best local scale modeling results but to understand how land surface processes simulated by todays LSMs drive the hydrological cycle on the seasonal time scale dependent on the climatic environment.

Results show that a latitudinal gradient in net radiation translates to a latitudinal gradient of the evaporative fraction, being lowest in the Mediterranean and highest in northern Europe. Extreme environmental conditions on the seasonal time scale, either dryness or coldness, require long term storage processes like soil heat and soil moisture storage to be part of the modeling system. Dry summer conditions in the Mediterranean require a biophysical (stomatal-) control of the water flux and also a storage capability for water in the root soil to hold this water for a prolonged period. Both processes are not present in the BUCKET model and it shows a poor performance in the Mediterranean. Modeling the land surface in northern Europe requires a soil heat scheme of monthly to seasonal storage capacity. BATS 1E and BUCKET, using a simple force-restore soil heat scheme, largely overestimated *LE* after the end of the growing season where not plant biophysics, but the surface heat balance drives surface fluxes. In central Europe the seasonal course of *LE* and *H* can be controlled by plant biochemistry and the timing and phase of vegetation phenology. In this case, the biophysical approach used in BATS 1E overestimates *LE* fluxes and underestimates *H* fluxes on the seasonal time scale, which is not the case for the photosynthesis-conductance model SiB 2.5.

Despite the difficulties encountered in parts of the driver data (the authors suggest that LW_d becomes part of the Fluxnet dataset), it was demonstrated that the integration of Fluxnet site measurements and land surface modeling is helpful in revealing and exploring missing processes of the hydrological cycle which could be relevant for coupled climate simulations. Runoff is a critical component of this cycle and largely varied by scheme. Therefore our future focus will be in using a similar modeling set-up to explore the catchment-scale soil moisture – runoff interaction, a scale where measurements of runoff are available and reliable.

Acknowledgements

The funding for this study was provided by the National Centre of Competence in Research on climate variability, predictability, and climate risks (NCCR Climate) funded by the Swiss National Science Foundation (NSF). The support of the ETH institute of Climate and Atmospheric Science and of Prof. Christoph Schär is gratefully acknowledged. We would like to thank to Richard Olson and Eva Falge for distributing the Fluxnet/Euroflux data and coordinating the Fluxnet project. Additional soil moisture and temperature data for this study was provided by Giorgio Matteucci (Collelongo site, JRC, Italy), Giampiero Tirone (Castel Porziano site, Unitus, Italy), Bernard Heinesch (Vielsalm site, FUSAGx, Belgium), Christian Bernhofer (Tharandt site, TU Dresden, Germany), Anders Lindroth and Harry Lankreijer (Norunda site, LU, Sweden), and Jon Gudmundsson (Gunnarsholt site, Agr. Res. Institute, Iceland). Thanks to Scott Denning (CSU) for the permission to use SiB2 and Mapper and to Jim Tucker, Jim Collatz and Sietse Los (NASA/GSFC) for their support on satellite remote sensing and land surface modeling.

References

Avissar R, Dias PLS, Dias MAFS, Nobre C (2002) The large-scale biosphere–atmosphere experiment in Amazonia (LBA): insights and future research needs. J Geophys Res-Atmos 107: 8086

Baker I, Denning AS, Hanan N, Prihodko L, Uliasz M, Vidale PL, Davis K, Bakwin P (2003) Simulated and observed fluxes of sensible and latent heat and CO_2 at the WLEF-TV tower using SiB2.5. Glob Change Biol 9: 1262–1277

Baldocchi D, Falge E, Gu L, Olson R, Hollinger D, Running S, Anthoni P, Bernhofer Ch, Davis K, Evans R, Fuentes J, Goldstein A, Katul G, Law B, Lee X, Malhi Y, Meyers T, Munger W, Oechel W, Paw U KT, Pilegaard K, Schmid HP, Valentini R, Verma S, Vesala T, Wilson K, Wofsyn S (2001) FLUXNET: A new tool to study the temporal and spatial variability of ecosystem-scale carbon dioxide, water vapor, and energy flux densities. Bull Amer Meteor Soc 82(11): 2415–2433

Betts AK, Ball JH (1997) Albedo over the boreal forest. J Geophys Res-Atmos 102: 28901–28909

Bonan GB (1996) A land surface model (LSM version 1.0) for ecological, hydrological, and atmospheric studies:

technical description and user's guide. NCAR Technical Note NCAR/TN-417 + STR, NCAR, Boulder, Colorado USA

Bounoua L, Collatz GJ, Los SO, Sellers PJ, Dazlich DA, Tucker CJ, Randall DA (2000) Sensitivity of climate to changes in NDVI. J Climate 13: 2277–2292

Buermann W, Dong JR, Zeng XB, Myneni RB, Dickinson RE (2001) Evaluation of the utility of satellite-based vegetation leaf area index data for climate simulations. J Climate 14: 3536–3550

Chen F, Pielke RA, Mitchell K (2001) Land surface hydrology, meteorology, and climate: observations and modeling. Water science and application, vol 3. Washington: American Geophysical Union

Chen TH, Henderson-Sellers A, Milly PCD, Pitman AJ, Beljaars ACM, Polcher J, Abramopoulos F, Boone A, Chang S, Chen F, Dai Y, Desborough CE, Dickinson RE, Dumenil L, Ek M, Garratt JR, Gedney N, Gusev YM, Kim J, Koster R, Kowalczyk EA, Laval K, Lean J, Lettenmaier D, Liang X, Mahfouf JF, Mengelkamp HT, Mitchell K, Nasonova ON, Noilhan J, Robock A, Rosenzweig C, Schaake J, Schlosser CA, Schulz JP, Shao Y, Shmakin AB, Verseghy DL, Wetzel P, Wood EF, Xue Y, Yang ZL, Zeng Q (1997) Cabauw experimental results from the project for intercomparison of land-surface parameterization schemes. J Climate 10: 1194–1215

Cox PM, Betts RA, Jones CD, Spall SA, Totterdell IJ (2000) Acceleration of global warming due to carbon-cycle feedbacks in a coupled climate model. Nature 408: 184–187

Dickinson RE, Berry JA, Bonan GB, Collatz GJ, Field CB, Fung IY, Goulden M, Hoffmann WA, Jackson RB, Myneni R, Sellers PJ, Shaikh M (2002) Nitrogen controls on climate model evapotranspiration. J Climate 15: 278–295

Dickinson RE, Henderson-Sellers A, Kennedy PJ (1993) Biosphere–atmosphere transfer scheme (BATS) version 1e as coupled to the ncar community climate model. NCAR Technical Note NCAR/TN-387 + STR, NCAR

Eastman JL, Coughenour MB, Pielke RA (2001) The regional effects of CO_2 and landscape change using a coupled plant and meteorological model. Glob Change Biol 7: 797–815

Falge E, Baldocchi D, Olson R, Anthoni P, Aubinet M, Bernhofer C, Burba G, Ceulemans R, Clement R, Dolmani H, Granier A, Gross P, Grünwald T, Hollinger D, Jensen N-O, Katulm G, Keronen P, Kowalski A, Lai CT, Law BE, Meyers T, Moncrieff J, Moorsi E, Munger JW, Pilegaard K, Rannik Ü, Rebmann C, Suyker A, Tenhunen J, Tu K, Verma S, Vesala T, Wilson K, Wofsy S (2001) Gap filling strategies for defensible annual sums of net ecosystem exchange. Agric Forest Meteorol 107: 43–69

Gedney N, Cox PM, Douville H, Polcher J, Valdes PJ (2000) Characterizing GCM land surface schemes to understand their responses to climate change. J Climate 13: 3066–3079

Heck P, Luthi D, Schär C (1999) The influence of vegetation on the summertime evolution of European soil moisture. Phys Chem Earth Pt B-Hydrol Oceans Atmos 24: 609–614

Henderson-Sellers A, Irannejad P, McGuffie K, Pitman AJ (2003) Predicting land-surface climates – better skill or moving targets? Geophys Res Lett 30: 1777

Holtslag AAM, Ek M (1996) Simulation of surface fluxes and boundary layer development over the pine forest in HAPEX-MOBILHY. J Appl Meteorol 35(2): 202–213

Idso SB (1981) A set of equations for full spectrum and 8-mu-m to 14-mu-m and 10.5-mu-m to 12.5-mu-m thermal-radiation from cloudless skies. Water Resour Res 17: 295–304

Koster RD, Suarez MJ (2001) Soil moisture memory in climate models. J Hydrometeorol 2: 558–570

Manabe S (1969) Climate and the ocean circulation. 1 the atmospheric circulation and the hydrology of the earth's surface. Mon Wea Rev 97(11): 739–774

McCaughey JH, Lafleur PM, Joiner DW, Bartlett PA, Costello AM, Jelinski DE, Ryan MG (1997) Magnitudes and seasonal patterns of energy, water, and carbon exchanges at a boreal young jack pine forest in the BOREAS northern study area. J Geophys Res-Atmos 102: 28997–29007

Moncrieff JB, Massheder JM, de Bruin H, Elbers J, Friborg T, Heusinkveld H, Kabat P, Scott S, Soegaard H, Verhoef A (1997) A system to measure surface fluxes of momentum, sensible heat, water vapour and carbon dioxide. J Hydrol 188–189: 589–611

Pielke RA (2001) Influence of the spatial distribution of vegetation and soils on the prediction of cumulus convective rainfall. Rev Geophys 39(2): 151–177

Pitman AJ, Henderson-Sellers A (1998) Recent progress and results from the project for the intercomparison of land-surface parameterization schemes. J Hydrol 213: 128–135

Running SW, Baldocchi DD, Turner DP, Gower ST, Bakwin PS, Hibbard KA (1999) A global terrestrial monitoring network integrating tower fluxes, flask sampling, ecosystem modeling and eos satellite data. Remote Sensing Environ 70: 108–127

Schär C, Luthi D, Beyerle U (1999) The soil-precipitation feedback: a process study with a regional climate model. J Climate 12: 722–741

Schmid HP, Su HB, Vogel CS, Curtis PS (2003) Ecosystem–atmosphere exchange of carbon dioxide over a mixed hardwood forest in northern lower michigan. J Geophys Res-Atmos 108: 4417

Sellers PJ, Dickinson RE, Randall DA, Betts AK, Hall FG, Berry JA, Collatz GJ, Denning AS, Mooney HA, Nobre CA, Sato N, Field CB, Henderson-Sellers A (1997a) Modeling the exchanges of energy, water, and carbon between continents and the atmosphere. Science 275(5299): 502–509

Sellers PJ, Hall FG, Asrar G, Strebel DE, Murphy RE (1988) The 1st ISLSCP field experiment (FIFE). Bull Amer Meteor Soc 69: 22–27

Sellers PJ, Hall FG, Kelly RD, Black A, Baldocchi D, Berry J, Ryan M, Ranson KJ, Crill PM, Lettenmaier DP, Margolis H, Cihlar J, Newcomer J, Fitzjarrald D, Jarvis PG, Gower ST, Halliwell D, Williams D, Goodison B, Wickland DE, Guertin FE (1997b) BOREAS in 1997: Experiment overview, scientific results, and future directions. J Geophys Res-Atmos 102: 28731–28769

Sellers PJ, Randall DA, Collatz GJ, Berry JA, Field CB, Dazlich DA, Zhang C, Collelo GD, Bounoua L (1996) A revised land surface parameterization (SiB2) for atmospheric GCMs. 1. Model formulation. J Climate 9: 676–705

Stöckli R, Vidale PL (2004) European plant phenology and climate as seen in a 20-year AVHRR land-surface parameter dataset. Int J Remote Sensing 25(17): 3303–3330

Vidale PL, Stöckli R (2004) Prognostic canopy air space solutions for SiB2 surface exchanges. Theor Appl Climatol (this issue)

Viterbo P, Beljaars A, Mahfouf JF, Teixeira J (1999) The representation of soil moisture freezing and its impact on the stable boundary layer. Quart J Roy Meteor Soc 125: 2401–2426

Wilson K, Goldstein A, Falge E, Aubinet M, Baldocchi D, Berbigier P, Bernhofer C, Ceulemans R, Doplman H, Field C, Grelle A, Kowalski A, Meyers T, Moncrieff J, Monson R, Oechel W, Tenhunen J, Valentini R, Verma S (2002) Energy balance closure at FLUXNET sites. Agric Forest Meteorol 113: 223–243

Authors' address: Reto Stöckli (e-mail: stockli@env.ethz.ch) and Pier Luigi Vidale (e-mail: pier-luigi.vidale@ethz.ch), Institute for Atmospheric and Climate Science, Winterthurerstrasse 190, 8057 Zürich, Switzerland.